Field instrumentation for performance assessment of Geobarrier System

Harianto Rahardjo[1,a], Zhai Qian[1], Alfrendo Satyanaga[1], Eng Choon Leong[1], Chien Looi Wang[2], Johnny Liang Heng Wong[2]

[1]*School of Civil and Environmental Engineering, Nanyang Technological University, 50 Nanyang Avenue, Singapore*
[2]*Building Research Institute, Housing and Development Board, HDB Hub, 460 Toa Payoh, Singapore*

Abstract: The saturated hydraulic conductivity of a coarse-grained material is normally higher than that of a fine-grained material. However, the unsaturated hydraulic conductivity of the coarse-grained material decreases much faster than that of the fine-grained material with increasing matric suction and consequently the coarse-grained material can be less permeable than the fine-grained material in unsaturated condition. A capillary barrier system with a fine-grained layer over a coarse-grained layer will act as a hydraulic barrier to minimize rainwater infiltration into the original soil. Geobarrier system (GBS) which can function as both a cover system (i.e. prevention of rainwater infiltration) and a retaining structure was designed and will be constructed at Orchard Boulevard in Singapore. Numerical simulations were carried out to determine the optimallocations of instruments that can be used to assess the performance of GBS during dry and wet periods. The monitoring results from tensiometers, earth pressure cells and weather station would be used to validate the results from the numerical analyses.

1 Introduction

Many factors can potentially determine slope failures, including climatic conditions, seismic activities, geological features, topography, vegetation and a combination of these factors [1]. In tropical regions, rainfall has been identified as the main cause of slope failures. Studies by Chowdhury et al. [2] indicated that the effects of rainfall have to be considered in landslide hazard assessments. Researchers have reported that most landslides occur in unsaturated residual soils during the wet season and they can potentially cause damages to infrastructure and human casualties [3, 4, 5]. Residual soils frequently exist in an unsaturated state in regions where the groundwater table is usually deep. Soil layers near the slope surface, which are initially unsaturated during dry seasons, have negative pore-water pressures, which are a major contributor to the shear strength of soils and to the stability of soil slopes. However during the wet seasons, rainwater infiltrates into the residual soil and increases the water content, thereby significantly increasing the pore-water pressures. Under these circumstances, the increase in pore-water pressure greatly reduces the shear strength of the soil. As a result, the slope may lose its original equilibrium and a slope failure will likely occur [6].

Singapore is located in the tropics where heavy rainfalls and high temperatures are conducive for rapid in-situ chemical and mechanical weathering that results in deep residual soil profiles. Because of the climatic conditions and geological features, slope instabilities are common in this region. To protect slopes against the possibility of rainfall-induced slope failures, preventive measures are necessary to ensure the safety of nearby buildings or public facilities. Capillary barrier system (CBS) is constructed on the surface of a slope in order to minimize rainfall infiltration into the slope and it can act as a slope preventive measure. A capillary barrier is an earthen cover system consisting of a fine-grained layer of soil overlying a coarse-grained layer of soil (Stormont, 1996). Previous research works have indicated the effectiveness of the capillary barrier system as a soil cover in reducing rainfall infiltration [7, 8, 9, 10, 11, 12).

The land space is very limited in Singapore. The construction of slopes with a steep inclination will have the advantage in intensifying of land usage. Previous studies by Rahardjo et al. [11, 12] indicated that CBS materials tend to slide down a steep slope surface if they are used solely as an added layer of slope cover system. Retaining structures are commonly used to retain the soil of a steep slope. Majority of materials that are used for the construction of retaining system comprise reinforced concrete or precast concrete elements, anchors embedded into soil and geosynthetic [13, 14]. In this paper, a new retaining structure that also acts as slope cover system, Geobarrier System (GBS) is presented. The GBS acts as earth retaining structure and slope cover by minimizing rainwater infiltration into the underlying soil layer. The surface materials of GBS can be vegetated to blend in with the surrounding environment.

Monitoring of slope is required to observe the current condition of the slope (stability, seepage, deformation) and to evaluate the effectiveness of slope preventive measures [15, 16, 17, 18]. Real-time monitoring will provide the early warning whether a slope is likely to fail or preventive measures are unsuccessful. It can also be

[a] Corresponding author: chrahardjo@ntu.edu.sg

used to verify the results of numerical analyses using finite element method. The collected data will also determine whether a single high value of measurement at a particular time is within a normal range for the instrumented slope. In this paper, the results from numerical analyses of slope supported with GBS are presented. The pore-water pressure variations from seepage analyses and the stress distributions from stress-strain analyses were used to determine the location of instruments that would be used to assess the performance of GBS in minimizing rainwater infiltration and retaining the lateral earth pressures of the soil from the steep slope.

2 Geobarrier System

Geobarrier system (GBS) consists of a fine-grained layer of material overlying a coarse-grained layer of material. The principle of the geobarrier system is based on the contrast in unsaturated hydraulic properties (soil-water characteristic curves and permeability functions) of these materials. Based on unsaturated soil mechanics theory, the coefficient of permeability as well as the water content of the coarse-grained soil can be much lower than that of the fine-grained soil at high suction values (Figure 1).

Under unsaturated conditions, the difference in permeability between the fine-grained layer and the coarse-grained layer limits the downward movement of water through capillary barrier effect. The mechanism of GBS can be explained using Figure 1b. At high matric suction values, the coefficient of permeability of the coarse-grained layer is much lower than that of the fine-grained layer. Under this condition, water will not flow into the coarse-grained layer. The infiltrated water is stored in the fine-grained layer by capillary forces. This infiltrated water is ultimately removed by transpiration, evaporation and lateral drainage through the slope or percolation into the drainage at the toe of the slope. When percolation (breakthrough) takes place, the capillary barrier no longer impedes water from infiltrating into the slope. Figure 2 shows the mechanism of GBS in minimizing the infiltration of rainwater into the slope.

In this study, a GBS will be constructed on a residual soil from Bukit Timah Granite in Singapore. Fine recycled concrete aggregate (RCA) will be used as the fine-grained material that will be placed inside Geobag within GBS whereas coarse RCA will be used as the coarse-grained material within GBS. In order to facilitate the planting of vegetation above GBS, the approved soil mixture (ASM) will be placed inside Geobag that will be placed as the most outer layer of GBS. Gravel layer will be placed at the bottom of GBS to drain out the water from GBS into the main surface drainage. The GBS will be constructed with 70 degrees of slope angle and 4 meters of slope height (Figure 3). The unsaturated properties which include the soil-water characteristic curves and permeability functions of ASM, fine and coarse RCA, and residual soil are presented in Figure 4.

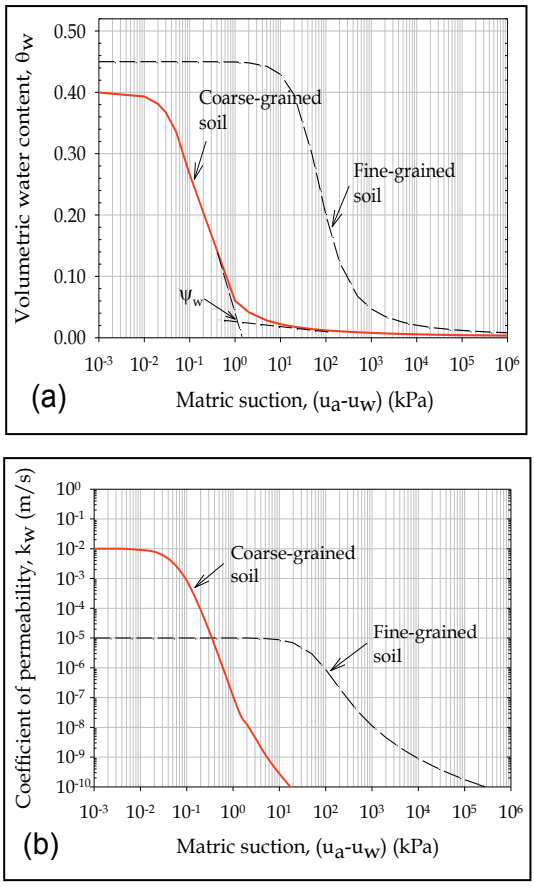

Figure 1. (a) Soil-water characteristic curves and (b) permeability functions of CBS materials

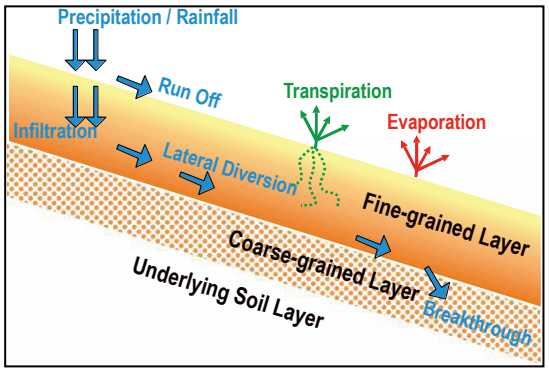

Figure 2. Capillary barrier system

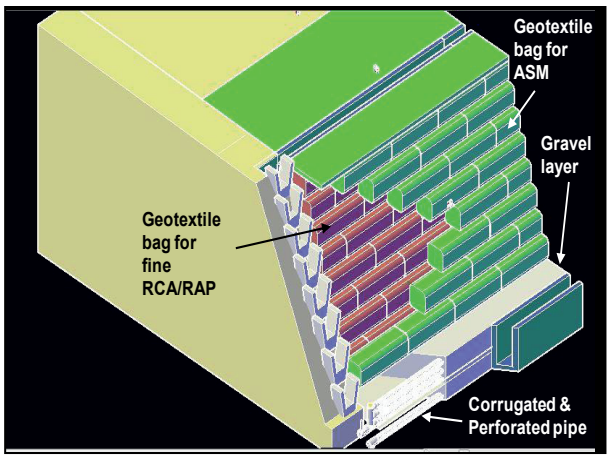

Figure 3. Schematic diagram of Gebarrier system

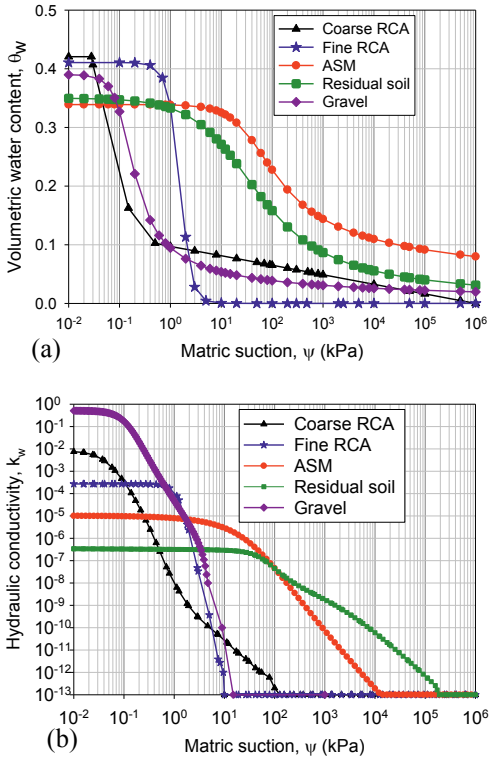

Figure 4. (a) SWCCs and (b) permeability functions of RCA, ASM and residual soil from Bukit Timah Granite

3 Numerical Analysis

Two-dimensional seepage analyses were carried out using finite element software, SEEP/W [19] and stress-strain analyses were conducted using SIGMA/W [20]. Two cases of numerical analyses were performed in this study. In the first case, the numerical model followed the geometry of the original slope consisting of a slope with an angle of 45 degrees and a height of 4 meters. In the second case, the numerical model followed the geometry of the GBS consisting of a slope with an angle of 70 degrees and a height of 4 meters. The groundwater table was observed at a depth of 1.86 meters and 4.54 meters below the ground surface on the top and bottom of the slope, respectively.

The boundary conditions applied to the finite element model are illustrated in Figure 5. The distance between the slope and the side of the slope model was set to three times the height of the slope to avoid the influence of the side boundary conditions. No flow boundaries were simulated by assigning a nodal flux, Q, equal to zero at the bottom and along the sides of the slope model above the groundwater table. A constant total head, hw, on each side was applied as the boundary condition along the sides of the slope model below the groundwater table. Rainfall was applied to the slope surface as a flux boundary, q. Ponding was not allowed to occur on the slope surface. This meant that when a flux greater than the permeability of the soil was applied to the top boundary, the seepage model would not allow pore-water pressures greater than 0 kPa to build up at the ground surface. This simulated the actual field conditions where the excess rainfall at the slope surface is removed as runoff.

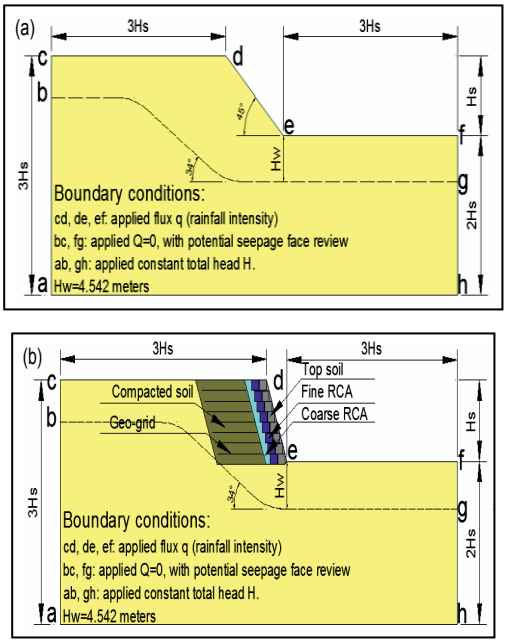

Figure 5. Geometries and boundary conditions of (a) existing slope with slope with slope angle of 45° and (b) 70° slope using GBS

The initial condition of the slope was taken based on the position of groundwater table in the field. The finite element model within the GBS and residual soil layer down to 5 m below the slope surface had a mesh size of approximately 0.5 m, smaller than elements in other parts of the slope, in order to obtain accurate results within the infiltration zone.

In the seepage analyses, a rainfall intensity of 18 mm/h was applied to the slope for 10 hours duration. The materials in the analyses were modelled as a linear elastic material. The parameters of materials and geo-grid used in the stress-strain analyses are summarized in Table 1. Several points within the numerical model were selected to illustrate the changes in pore-water pressures and stress with time as obtained from the seepage and the stress-strain analyses of cases 1 and 2 (Figures 6 and 7, respectively). Points TA and TC were located within the fine-grained layer, point TB was located within the residual soil below the GBS layer, point TD was located within the coarse-grained layer.

The Young's Modulus and Poisson ratio of soils were summarized in Table 1. Pore-water pressures computed from SEEP/W were incorporated into SIGMA/W to calculate the stress in a selected position in three directions (i.e., x, y, z directions).

Table 1. Parameters of materials and Geo-grid used for stress-strain analysis

Soil Description	γ (kN/m^3)	E (kPa)	μ
Approved soil mixture	18	5000	0.45
Fine RCA	20	120000	0.35
Coarse RCA	21	200000	0.35
Residual soil	18	6000	0.40
Gravel	21	200000	0.34
Precast drain	24	200000	0.34

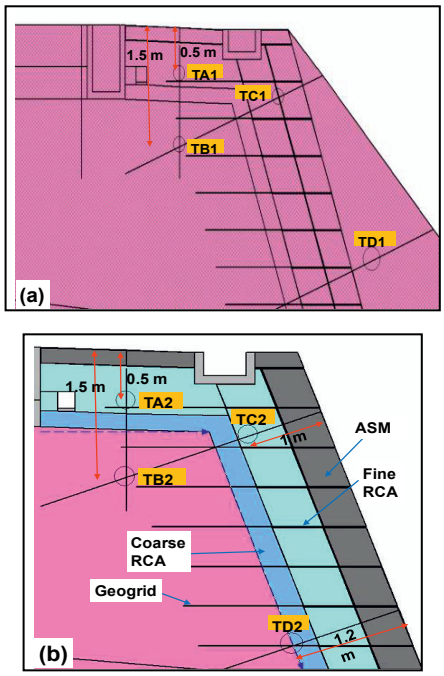

Figure 6. Location of points within GBS and residual soil for monitoring of pore-water pressure variations within (a) original slope and (b) slope retained with GBS during and after rainfall

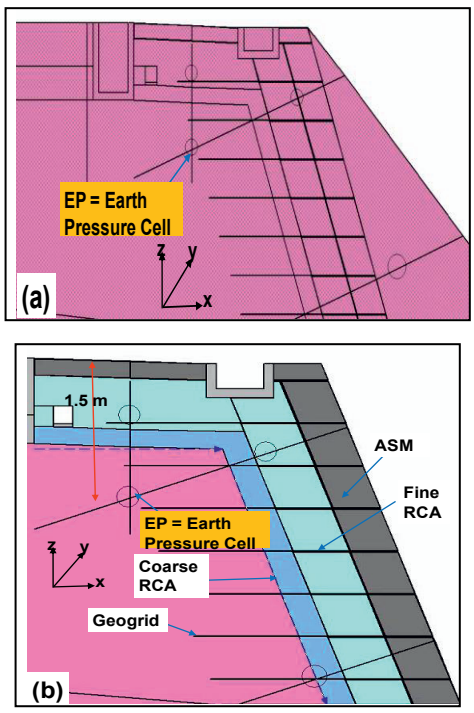

Figure 7. Location of point EP within GBS and residual soil for monitoring of lateral earth pressure within (a) original slope and (b) slope retained with GBS during and after rainfall

4. Results and Discussions

The pore water pressures variations with time at points TA, TB, TC and TD (see Figure 6) from the seepage analyses of case 1 (original slope) and case 2 (slope retained with GBS) are shown in Figures 8 and 9. Figure 8a shows that the pore-water pressure at point TA1 within the original slope increased significantly during rainfall and decreased after rain stopped. On the other hand, the pore-water pressure at point TA2 at the bottom of fine RCA within the slope retained with GBS remained constant around -65 kPa during rainfall. This indicated that GBS performed well in reducing rainwater infiltration into the underlying soil layer below GBS. Tensiometers and soil moisture sensors can be installed at point TA to assess the performance of GBS and to verify the results from the seepage analyses at the crest of the slope during and after rainfall. Figure 8b shows that the pore-water pressure at point TB1 within the original slope increased significantly during rainfall and decreased after rain stopped. On the other hand, the pore-water pressure at point TB2 within the residual soil behind GBS increased gradually from – 55 kPa to – 20 kPa during rainfall. This indicated that the surface drainage behind the GBS layer at the crest of the slope was deep enough to avoid the excessive increase in pore-water pressure behind GBS. Tensiometers and soil moisture sensors can be installed at point TB to assess the performance and to validate the results of seepage analyses of the surface drainage behind GBS at the crest of the slope.

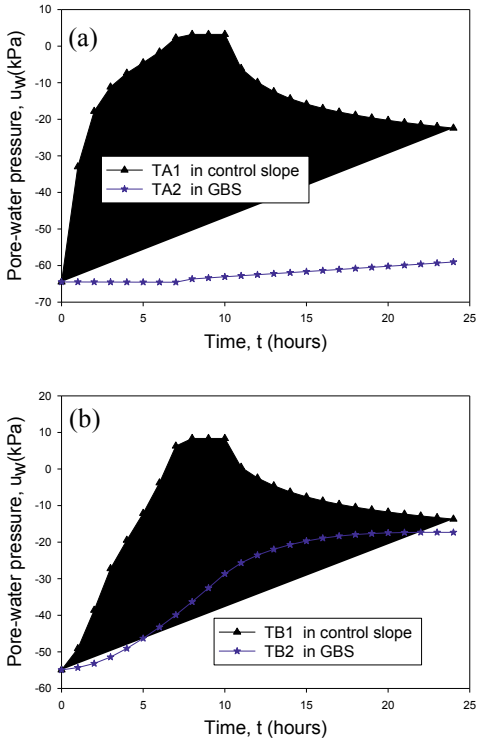

Figure 8. Variations of pore-water pressures with time at points (a) TA and (b) TB within original slope and slope retained with GBS

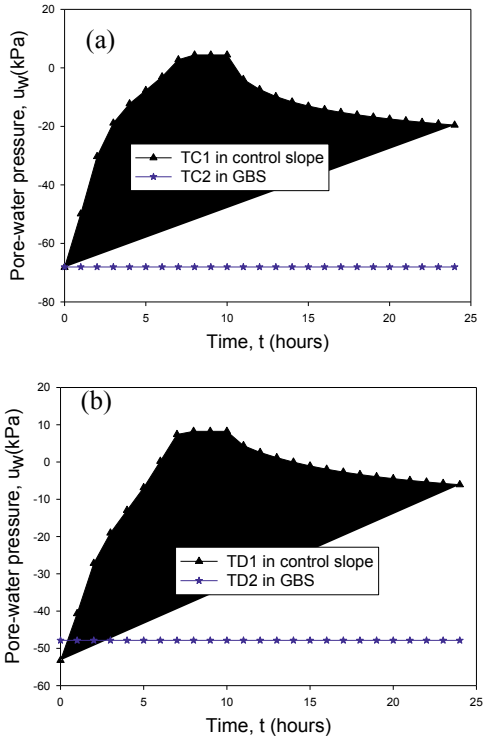

Figure 9. Variations of pore-water pressures with time at points (a) TC and (b) TD within original slope and slope retained with GBS

Figs 9a and 9b show that the pore-water pressures at point TC1 and TD1 within the original slope increased significantly during rainfall and decreased after rain stopped. On the other hand, the pore-water pressure at point TC2 and TD2 at the bottom of fine RCA and at the bottom of coarse RCA, respectively, within the slope retained with GBS remained constant around -70 kPa and -48 kPa, respectively during and after rainfall. This indicated that GBS performed well in reducing rainwater infiltration into the underlying soil layer below GBS. Tensiometers and soil moisture sensors can be installed at points TC and TD to assess the performance of GBS and to validate the results from the seepage analyses of GBS comprising fine RCA and coarse RCA layers during and after rainfall.

Total stresses at point EP in x, y and z directions within the original slope and the slope retained with GBS (Figure 7) were plotted against pore-water pressures and presented in Figure 10. Figure 10 indicates that total stresses in all directions remained constant when the pore-water pressures were negative. On the other hand, total stresses in all directions increased drastically when the pore-water pressures became positive. In the original slope, the soil was saturated by the infiltrated rainwater and total stresses in all directions increased significantly after 6 hours of rainfall. On the contrary, the soil under the GBS remained in unsaturated condition during the rainfall period and there were no changes in total stress. As the non-linear contributions from matric suction to effective stress are not yet accommodated by SIGMA/W, the total stress computed from SIGMA/W in this study did not incorporate the effect of changes in suction. However, the results from SIGMA/W can describe the differences in total stresses between soils with and without suction as presented in Figure 10. Figure 10 indicates significant changes in total stresses at point EP in Figure 7 for the soil within the original slope. As a result, the earth pressure cell can be installed at point EP in the original slope and in the slope retained by GBS to illustrate the effectiveness of GBS during rainfall.

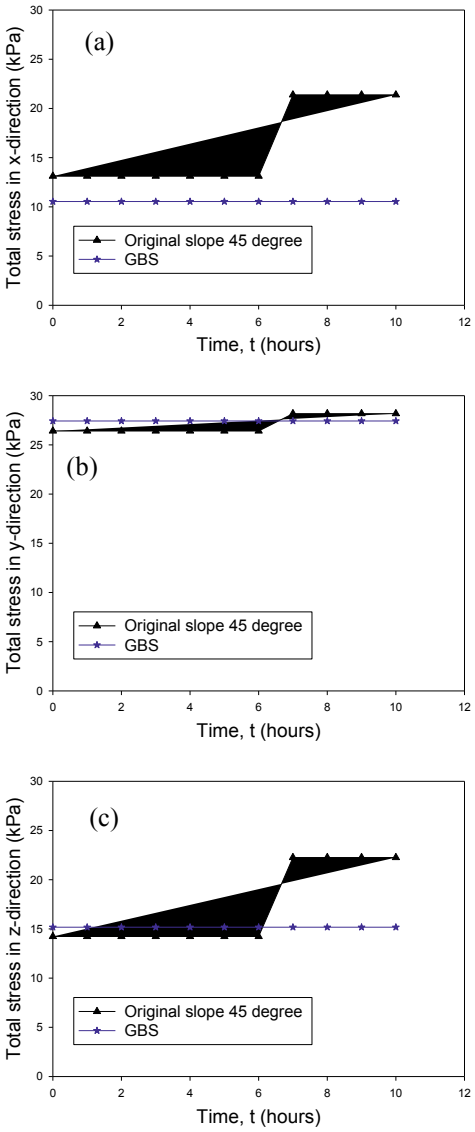

Figure 10. Variations of total stress with pore-water pressures in (a) x-direction, (b) y-direction and (c) z-direction within original slope and slope retained with GBS

5 Locations of Instruments

Numerical analysis results indicated that the proposed locations of tensiometers (TA, TB, TC and TD) as shown in Figure 6 were appropriate for monitoring the pore-water pressures changes due to rainwater infiltration. In addition, earth pressure cells should be located at the proposed location EP as shown in Figure 7 to monitor the stress changes due to rainwater infiltration. In the field, three slopes will be retained with GBS consisting of different types of recycled materials (Figure11). Slope 1 will comprise fine and coarse recycled concrete aggregate (RCA) as fine- and coarse-grained materials within GBS,

respectively. Slope 2 comprises fine and coarse reclaimed asphalt pavement (RAP) as fine- and coarse-grained materials within GBS, respectively. Slope 3 comprises fine RCA and coarse RAP as fine- and coarse-grained materials within GBS, respectively. Slope 4 is an original slope that will be used as a reference slope.

Tensiometers (TA, TB, TC and TD) and earth pressure cells (EPA at x-direction, EPB at y-direction, EPC at z-direction) will be installed at the same depth in the proposed locations shown in Figures 6 and 7. In addition, soil moisture sensors (SA, SB, SC and SD) will be installed following the same arrangement as those for tensiometers (Figure 11). Two piezometers will be installed at the crest and toe of the slope to monitor the variations of groundwater table during dry and wet periods. A weather station will be installed near the toe of the slope to monitor the variations of rainfall and evaporation with time.

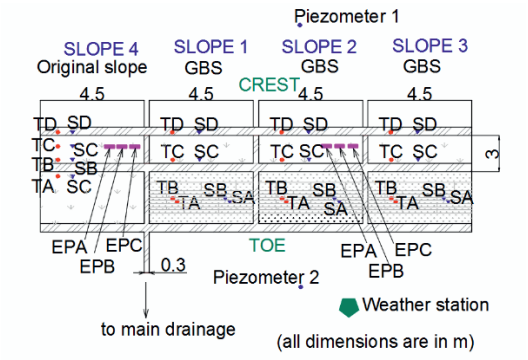

Figure 11. Proposed plan view of field instrumentation for assessment of GBS

6 Conclusions

A new slope protection system named as Geobarrier system (GBS) is proposed from this study. The GBS can be used as a retaining structure that utilizes capillary barrier mechanism for controlling rainfall infiltration into the original soil behind the retaining structure. The results of the numerical analyses indicated the optimal locations for tensiometers, soil moistures sensors and earth pressure cells within the original slope and the slope retained with GBS. The monitoring results of the instruments can be used to assess the performance of GBS as a retaining structure and slope stabilization system.

Acknowledgement

The findings published in this paper are based on the project "GeoBarrier System for Use in Underground Structure" (Grant No. SUL2013-3) that is supported by a research grant from the Ministry of National Development Research Fund on Sustainable Urban Living, Singapore

References

1. A. Basile, G. Mele, F. Terribile. Geoderma, **117**, 3-4, 331-346 (2003)
2. R. Chowdury, P. Flentje, G. Bhattacharya. *Geotechnical Slope Analysis* (2010)
3. D.G. Fredlund, H. Rahardjo. *Soil Mechanics for Unsaturated Soils*, pp. 517 (1993)
4. H. Rahardjo, A. Satyanaga, E.C. Leong, Y.S. Ng. J Geo & Geoenviro Eng, ASCE, **136**, 11, 1555–1564 (2010)
5. H. Rahardjo, A. Satyanaga, E.C. Leong. J. Eng. Geo., Special Issue on Unsaturated Soils: Theory and Applications, **165**, 133-142 (2013a)
6. D.G. Fredlund, H. Rahardjo, M.D. Fredlund. *Unsaturated Soil Mechanics in Engineering Practice*, 926 pp (2012)
7. C.E. Morris, J.C. Stormont. J. Envir. Engrg., ASCE, **123**, 1, 3-10 (1997)
8. M. Khire, C. Benson, P. Bosscher. J. Geo. Geoenvir Eng., ASCE, **126**, 8, 695-708 (2000)
9. D. Tami, H. Rahardjo, E.C. Leong, D.G. Fredlund. Geo. Test. J., ASTM, **27**, 2, 173-183 (2004a)
10. D. Tami, H. Rahardjo, E.C. Leong, D.G. Fredlund.. Can. Geo. J., **41**, 5, 814 – 830 (2004b)
11. H. Rahardjo, V.A. Santoso, E.C. Leong, Ng., Y.S. C.J. Hua. J. Geo. & Geoenvi Eng., **138**, 4, 481 – 490 (2012)
12. H. Rahardjo, V.A. Santoso, E.C. Leong, Y.S. Ng, C.P.H. Tam, A. Satyanaga. Can. Geo. J., **50**, 1-12 (2013b)
13. AASHTO. *Standard Specifications for Highway Bridges*, 7th ed., 689 (2002)
14. NCMA. *Design Manual for Segmental Retaining Walls,* 3rd ed., 282 (2010)
15. J. Gasmo, K.J. Hritzuk, H. Rahardjo, E.C. Leong. Geo. Test. J., **22**, 2, 128-137 (1999)
16. G. Gitirana Jr., D.G. Fredlund, M.D. Fredlund. Proc. 58th Can. Geo. Conf., 516-523 (2005)
17. H. Rahardjo, V.A. Santoso, E.C. Leong, Y.S. Ng, C.J. Hua. Soils and Foundations, **51**, 3, 471-482 (2011)
18. H. Rahardjo, A. Satyanaga, E.C. Leong, J.-Y. Wang Procedia Earth and Planetary Science, **9**, 23-43 (2014)
19. Geoslope International Ltd., *Seep/W User's Guide for Finite Element Analysis*. (2007a)
20. Geoslope International Ltd., *Sigma/W User's Guide for Finite Element Analysis,* (2007b)